Void Fraction Measurement of Gas-Liquid Two-Phase Flow Based on Empirical Mode Decomposition and Artificial Neural Networks

Void Fraction Measurement of Gas-Liquid Two-Phase Flow Based on Empirical Mode Decomposition and Artificial Neural Networks

Weiwei Wang[1], Khellil Sefiane[2,3], Gail Duursma[2*] , Xiao Liang[1], Yu Chen[1]

[1]College of Information and Control Engineering, China University of Petroleum (East China), Qingdao 266580, China

[2]School of Engineering, The University of Edinburgh, Kings Buildings, Mayfield Road, Edinburgh EH9 3JL, UK

[3]International Institute for Carbon-Neutral Energy Research (I2CNER) Kyushu University, 744 Motooka, Nishi-ku, Fukuoka 819-0395

[*]Address correspondence to Dr Weiwei Wang, College of Information and Control Engineering, China University of Petroleum (East China), Qingdao 266580, China Email: wangww@upc.edu.cn Or Dr Gail Duursma, School of Engineering, The University of Edinburgh, The King's Buildings, Mayfield Road, Edinburgh EH9 3JL, UK E-mail: gail.duursma@ed.ac.uk Phone Number: 0 (+44) 131 650 4868, Fax Number: 0 (+44) 131 650 6551

ABSTRACT

A new void fraction estimation method for gas-liquid two-phase flow combining two differential pressure (DP) signals acquired from a single Venturi tube and based on Empirical Mode Decomposition (EMD) and Artificial Neural Networks (ANN) was experimentally investigated. In order to study gas-liquid distribution in horizontal pipes, two DP signals from the top and bottom sections of the Venturi tube are acquired and EMD is adopted to extract stable and fluctuating components of the DP signals. Experimental data revealed that fluctuating index increases nearly linearly with increasing void fraction when void fraction is less than 0.4. When void fraction is larger than 0.4, this near-linearity ceases. A combination of ANN method and the fluctuating index of DP signals is developed to estimate void fraction. Experimental results show that void fraction based on DP signal from top section of Venturi tube is overestimated because of clustering of bubbles and the scarcity of liquid information when gas-liquid mixture velocity is low. Void fraction is underestimated when the mixture velocity is high. A high gas-liquid slip ratio results in void fraction underestimation. Void fraction prediction performance is satisfactory when void fraction is less than 0.4 and fluctuating index of DP signal less than 1.2.

INTRODUCTION

Accurate void fraction measurement of multiphase flow is of great importance in many industrial fields (Kawahara *et al.*[1]. Together with pressure variation and mass transfer, bubble coalescence and break-up in gas-liquid two-phase flow are responsible for changes in bubble sizes and void fraction (Hewitt and Burnout [2]; Hosokawa and Tomiyama, [3]. Gas-liquid two-phase flow has inherent complexity, which leads to the difficulty of void

fraction measurement. Research on the topic, mainly including direct measurement and indirect measurement methods, is described in Sharaf *et al.* [4].

Among the direct void fraction measurement methods, the most common one is the so-called quick-closing valve method. It requires quickly shutting down two quick-closing valves installed in the pipe when a stable flow status in the measurement section is observed. Thereafter, the gas in the pipe is discharged and the volume of residual liquid is measured. Finally, knowing the volume of the measuring section, the volume-average void fraction between the two valves can be calculated. Although this procedure is accurate, it is unable to achieve real-time online measurement because of the need artificially to cut off the normal flow of fluid in the pipe, and this limits its onsite application in actual industrial production. At present, this method is mainly suitable for laboratory research on void fraction and the calibration of void fraction measurement devices (Li [5]). In addition, void fraction estimation and analysis based on other techniques in a wide range of fields have been studied (Cioncolini and Thome [6]; Celata *et al*. [7]; Meng *et al*. [8]). Srisomba *et al.* [9] proposed new correlations to predict the void fraction by combining the vapour quality and the physical properties of R-134a refrigerant in a horizontal tube using a quick-closing valve and optical observation techniques. The experimental results showed that the presented correlations could predict void fraction with mean relative error within 20% for intermittent, wavy and annular flow patterns. The correlations (Srisomba *et al*. [9]) are different for the three flow patterns above. Kim *et al.* [10] proposed a capacitance method to measure the space-averaged void fraction in concentric annular flows, derived the expression for the capacitance in terms of a given void fraction, and developed a closed-form formula to predict the void fraction from

capacitance measurements. Uesawa *et al.* [11] proposed a void fraction estimation method for three-dimensional dispersed bubbly flow based on Maxwell's theory and polarization of tiny bubbles whereas Jassim and Newell [12] developed probabilistic two-phase flow map models to predict void fraction and pressure drop for R134a, R410A and air-water in 6-port microchannels. Lewis *et al.* [13] analysed the nature of the voltage signals acquired from a probe and proposed a signal processing scheme for measurement of time-averaged void fraction of small and large bubbles for a horizontal slug flow pattern in a 50.3 mm i.d. pipe. Milian *et al.* [14] studied the influence of different mean void fraction correlations on the performance of condensers using R134a as working fluid under different main operating variables. The study showed the significance of the mean void fraction correlation on the condenser model predictions with noticeable discrepancies depending on the correlation used. A performance comparison of 68 void fraction correlations from different studies covering a wide parameter range was given by Woldesemayat and Ghajar [15], and the results showed that most of the correlations are restricted in terms of handling a wide variety of data sets.

In recent years, the relationships between differential pressure (DP) signals caused by throttling element formation and the discrete phase concentration have been investigated and many results have been reported (Fang *et al*., [16]). Lao [17] analysed the relationship between the fluctuating parameter $p_f = SD/\Delta P_{TP}$ and the void fraction α. SD denotes the standard deviation of the DP fluctuation signal, and ΔP_{TP} denotes the average of the DP fluctuation signal in a horizontal pipe. Lao [17] derived the following equation for the fluctuating parameter:

$$p_f^{\,2} = \frac{k_1(\alpha) - (1-\alpha)^{l-4}}{(1-\alpha)^{l-5}} + \frac{k_2(\alpha) - \alpha^{l-4}}{\alpha^{l-5}} \tag{1}$$

where l is index determined based on experimental data, $k_1(\alpha)$ and $k_2(\alpha)$ are empirical functions dependent upon experimental conditions and α. According to Eq. (1), provided that l is known, p_f can be estimated based on the value of α and Eq. (1). But in reality, determining l is not straightforward. Eq. (1) is developed from the experiments in which void fraction value was less than 0.5. So, when the void fraction value is larger than 0.5, Eq. (1) is no longer valid.

Two-phase flow measurement using a Venturi meter is widely reported because of its advantages, including the short straight pipe length, small pressure loss, small flow pattern interference (Bertoldi *et al*. [18]; Steven [19]; Sun *et al*. [20]), small vibration noise disturbance, and large DP signal amplitude (Steven [21]). Recently, some researchers (Sun *et al*. [20]; Zhang *et al*. [22]) claimed that DP fluctuation signals contain some additional information related to gas-liquid two-phase distribution, hence the DP signals measured from a Venturi tube could lead to void fraction estimation when combined with the measurement model.

Zhang *et al*. [22] analysed the influence of mass flowrate, pressure, void fraction and density on DP signals, and provided a relationship between void fraction of gas-liquid two-phase flow and root-mean-square deviation of the DP fluctuating signals acquired from a Venturi tube. The following expression is deduced:

$$\frac{D}{\Delta P_{TP}} = c\left(\frac{\Delta P_{TP}}{P}\right)^{-0.5} \alpha^a (1-\alpha)^b \qquad (2)$$

where D is the variance of DP signal, a,b,c are coefficients to be determined under experimental conditions, P denotes the average pipe pressure before the Venturi tube. In this method, it is necessary to determine the values of a,b,c according to the experimental

reference void fraction before measurement. Online void fraction measurement can be achieved by using the correlation and the DP signal acquired from the Venturi tube. Although many studies have been carried out to build a correlation between DP information and void fraction in a two-phase mixture, no general correlation presently predicts the void fraction accurately for various flow patterns.

In horizontal gas-liquid two-phase flow, the thicker liquid film at the bottom of a bubble or slug unit occurs with increasing gravity, resulting in a larger void fraction in the top layer of the pipes and a longer region with zero void fraction in the bottom layer (Liu *et al*. [23]; Colin *et al*. [24]). Meanwhile, owing to the strong influence of buoyancy, the migration of dispersed bubbles towards the top wall of the horizontal pipe generally causes a highly asymmetrical internal phase distribution, and hence the void fraction reaches a maximum near the top wall of the pipe due to buoyancy (Yeoh *et al*. [25]). Because there exists a significant influence of gravity and buoyancy on the phase distribution of horizontal gas-liquid two-phase flow (Liu *et al*. [23]; Colin *et al*. [24]; Yeoh *et al*. [25]), a partial DP signal from certain location of Venturi tube cannot reflect the gas-liquid distribution comprehensively and accurately. Hence, DP signals from different locations of one Venturi tube should be considered to provide more information related to gas-liquid distribution. The objective of this study is to analyse the influence of gas-liquid distribution on the fluctuations of DP signals acquired from the top and bottom sections of one Venturi tube, to analyse the void fraction prediction performance according to individual DP signals, and finally to find a solution in order to estimate the void fraction more accurately by combining two DP signals. Empirical mode decomposition (EMD) and Artificial Neural Networks (ANN) were chosen for analysis

because of the good nonlinear mapping capability of this methodology.

EXPERIMENTAL FACILITY

A series of experiments was carried out in State Key Laboratory of Industrial Control Technology in Zhejiang University using the experimental facility shown in Fig. 1. Air and water were used as working fluids. Air is supplied from GX-7FF air compressor produced by Wuxi Atlas Copco Compressor Co. Compressed air flows into a surge tank with 0.4 MPa pressure, and then flows through a calibrated Vortex flowmeter into a two-phase mixer. The Vortex flowmeter is from Henghe Electric Machinery Co., Ltd. Water is supplied from a pump and flows through a calibrated Electromagnetic flowmeter into the two-phase mixer. Gas and liquid phases are mixed through a horizontally installed baffle plate.

Before flowing into the test section, the gas-liquid mixture passed through a straight pipe to ensure a fully developed flow pattern. In this work, the pipe diameter is 40 mm, and the straight pipe before the test section is 15 m long to ensure the flow pattern development. The rotameter with 1.0 % accuracy and Vortex flowmeter with 1.0 % accuracy are used to measure the gas reference flowrate before mixing. The Electromagnetic flowmeter with 1.0 % accuracy is used to measure the liquid reference flowrate before mixing. The Electromagnetic flowmeter is from Shanghai Guanghua Emmett Co. Ltd. After the mixer, flow is two-phase. Two valves are located before the Venturi tube for the reference void fraction measurement. When the flow is stable, two valves shut down simultaneously. At this moment, a section of gas-liquid mixture is blocked between two valves. The liquid is released from the bottom of the pipe and the volume of the liquid is measured. The volume difference between the liquid and the gas-liquid mixture divided by the volume of the gas-liquid mixture is the reference void fraction. After leaving the test section, the two-phase mixture was separated by a gas-liquid separator. Then air was discharged to atmosphere, while the water flowed into a water tank for recycling.

The Venturi tube is installed horizontally in the test section. The Venturi tube is produced by Hangzhou throttling device Co., Ltd. The internal diameter and external diameter of the Venturi tube are 40mm and 46mm, respectively. The ratio of diameter of the Venturi throat to pipe is 0.58 and the accuracy is 1.0 %. Fig. 2 illustrates the Venturi structural parameters and the positions of the pressure taps on the outer-wall along the Venturi tube and those on the cross section of the Venturi tube. The pressure taps are located upstream of the converging cone and at the middle of the throat. Two Rosemount 3051 DP transducers acquire the DP signals from the top and the bottom sections of the Venturi tube, as shown in Fig 2(b). The DP signals were fed to a computer for processing through an A/D converter. During the test, the pipe pressure was varied from 0.25 MPa to 0.40 MPa, the gas mass flowrate ranged from 0.003 kg/s to 0.021 kg/s, the liquid mass flowrate ranged from 1.02 kg/s to 4.22 kg/s, the void fraction ranged from 0.1277 to 0.7490, the quality ranged from 0.00114 to 0.0197, and three kinds of flow patterns namely bubble flow, plug flow and slug flow were observed.

RESULTS AND ANALYSIS

Characteristic variables based on Empirical Mode Decomposition

Fig. 3(a) and Fig. 3(b) illustrate typical DP signals, ΔP_{top} and ΔP_{bottom}, which are acquired from the top section and the bottom section of the Venturi tube, respectively. To analyse the connections between the DP signals and the void fraction, the fluctuating components and the residual component are calculated based on EMD, as shown in Fig. 4.

According to the EMD principle (Huang *et al*. [26]), the Intrinsic Mode Functions (IMFs) of DP signal are essentially the fluctuating components of DP signal, and the residue is the

mean component of DP signal or the stable part of DP signal. Previous studies indicated that the variance and the mean value of DP signal played an important role in void fraction estimation. Therefore, by combining the fluctuating and stable components of DP signal it would be possible to estimate the void fraction.

The EMD method decomposes the original signal to the fluctuating components, residual component and pseudo-components. Pseudo-components are derived from the energy leakage in the EMD process. The small difference between the actual analogue signal and the corresponding discrete signal leads to a minor deviation between the actual extreme points and the extracted ones. This minor deviation generates an energy leakage, and hence the induced pseudo-components emerge with low frequency and low energy. Therefore, the pseudo-components can be regarded as near-stable components.

Based on the components from EMD, the fluctuating variable, F, and the stable variable, R, are defined according to the following:

$$F = \sqrt{\frac{1}{m}\sum_{i=1}^{m} x_i^{\,2}} \tag{3}$$

$$R = \frac{1}{n}\sum_{j=1}^{n}(r + c_j) \tag{4}$$

where x_i represents the fluctuating component of DP signal, r represents the residual component of DP signal and c_j represents the pseudo-components. m and n denote the number of the fluctuating components and the pseudo-components, respectively. Further, the dimensionless fluctuating index d is defined as:

$$d = \frac{F}{R} \tag{5}$$

The EMD method is based on the eigenmodes of the signal, so F, R and d can reflect the essential characteristics corresponding to the original signal. Using these

characteristic variables to estimate the void fraction should yield good results.

Two DP signals, ΔP_{top} and ΔP_{bottom}, are acquired from the top section and the bottom section of the Venturi tube, (Fig. 2). Characteristic variables, $F_{top}, R_{top}, d_{top}$ and $F_{bottom}, R_{bottom}, d_{bottom}$, are calculated from ΔP_{top} and ΔP_{bottom} according to equations (3)-(5). Figs. 5 and 6 illustrate the relationships between the dimensionless variable d and the void fraction α under different liquid flowrate for ΔP_{bottom} and ΔP_{top}.

Figs. 5 and 6 show that there exists a consistent relationship between d and α. Under certain liquid flowrates, d increases monotonically with increasing void fraction, an exhibits near-linearity when void fraction is less than 0.4. When void fraction is larger than 0.4, this near-linearity ceases. Furthermore, d decreases with the increasing liquid flowrate for a constant void fraction.

Considering the flow, for conditions of the same void fraction value or similar gas-liquid distribution in the pipe, the flow characteristics are basically identical, and the fluctuating components of the DP signal are also basically similar.

The residue reflects the stable component of the DP signal. In horizontal gas-liquid two-phase flow, due to the effect of gravity, the liquid phase mainly distributes at the bottom of the pipe. Previous research showed that the characteristics of the liquid phase are mainly reflected on the stable component of the DP signal (Sun [27]). i.e., the characteristics of the liquid phase are mainly described by the residue of the DP signal. Therefore, *R* increases with increasing liquid flowrate. In view of Eq. (5), for a constant void fraction value corresponding to constant *F*, the increase in *R* will inevitably lead to a decrease in *d*.

Fig. 6 is similar to Fig. 5, however, the values in Fig. 6 are much more scattered and the

values of d are larger than those in Fig. 5 for the same void fraction value. The reason for this is that R values calculated from ΔP_{top} are overall smaller than those from ΔP_{bottom}, and F values calculated from ΔP_{top} are generally larger than those from ΔP_{bottom}.

In conclusion, the nonlinear relationship between α, d and R is unambiguous but is difficult to quantify. Nonlinear mapping may perhaps be a good choice to describe the relationship between the variables. Artificial Neural Networks also has a good nonlinear mapping capability. In what follows we will use ANN model to map the connections between α, d and R.

ANN modelling

ANN is one of the statistical learning algorithms inspired by biological neural network and are used to estimate or approximate the complicated functions which depend on a large number of parameters. An ANN is generally presented as a system of interconnected "neurons" which send messages to each other. The connections between the neurons have numerical weightings which can be tuned based on the experimental data.

ANN is a nonlinear modeling tool, which models the complex relationships between inputs and outputs or elucidates the mode between data (Hornik *et al*. [28]). The criterion to evaluate the performance of an ANN model is not the learning ability of the training sample data, but the ability to accurately predict new data, which is called the generalization ability. To a certain extent, the generalization ability is also improved with the improvement of the learning ability, but this can be hampered by over-fitting.

Disrupting the order of the input data can make the data appear more typical, which is good for improving the generalization ability of the model. One way to avoid over-fitting is

the training early stop method. This method will randomly separate the sample data into three parts: a training data set, a validation data set and a test data set. There is no overlap between these.

The training data set is used to train neural network. After each training, the validation data set will automatically be input to the neural network to validate the generalization ability and an error will be output after validation. The network system will choose the optimal model according to the error change. Once the output error reaches the minimum, the network system will stop training automatically in order to prevent over-fitting, and hence the network model is determined. Clearly, the training set is used to generate the model, the validation set is used to find the network optimal weights and thresholds, and the test set is used to check the prediction accuracy of the network.

In this work, part of the experimental DP data are chosen to model the neural network. Then the developed neural network is used to predict the void fraction of gas-liquid two-phase flow. The experimental working conditions are shown in Fig. 7.

The experimental working conditions in Fig. 7 involve three kinds of flow patterns including bubble flow, plug flow and slug flow. The training data comprised 102 sets of conditions were examined and were used to build the neural network. The void fraction corresponding to the other 33 sets of conditions are estimated based on the built neural network.

Based on the training data in Fig. 7, the mean square errors calculated based on the training data, the validation data and the test data versus the number of iterations are shown in Fig. 8. The training errors decrease sharply in the initial stage of iteration and then settle at the

later stages of iteration. The validation errors also decrease sharply in the initial stage of iteration but then increase with the iterations. This indicates that the redundant iterations make the ANN contain too much individual information and hence the generalization performance of ANN decreases. The turning point in Fig. 8 corresponds to the best training performance and the ANN model corresponding to this point has the best generalization ability.

Mean square error (*MSE*) is computed as follows:

$$MSE = \frac{1}{N}\sum_{i=1}^{N}(output - target)^2 \quad (6)$$

where *output* represents the output prediction value of neural network model, *target* represents the output reference value, and N denotes the number of working conditions for prediction.

Void fraction estimation based on one DP signal

In order to assess the overall prediction accuracy, the average relative error ε is defined as:

$$\varepsilon = \frac{1}{N}\sum_{i=1}^{N}\frac{|output - target|}{target} \times 100\% \quad (7)$$

The relative error, RE, calculated for assessing the prediction accuracy of each sample, is defined as:

$$RE = \frac{output - target}{target} \times 100\% \quad (8)$$

According to the analysis above, there exists a nonlinear relationship between the fluctuating index, the stable variable and the void fraction. These variables are input into the developed neural network to predict the void fraction. The experimental reference void fraction is set as the desired output of the neural network. The neural network structure is shown in Fig. 9. It is a three-layer feed-forward network with 20 hidden layer nodes, 2 inputs, 1 output, a sigmoid activation function in the hidden layer and a linear activation function in

the output layer.

d_{top}, R_{top} and d_{bottom}, R_{bottom} are regarded as the input vector of the neural network to predict the void fraction. The average relative errors of void fraction prediction based on ΔP_{top} and ΔP_{bottom} are 10.05 % and 12.46 %, respectively. The relative error of each sample is shown in Figs. 10(a) and (b).

In Fig. 10(a), it is shown that the relative errors are within 10 % and a good prediction accuracy can be achieved when the void fraction is less than 0.4. When the void fraction is larger than 0.4, larger errors appear. The conditions with larger errors are found to correspond to slug flow and plug flow.

Compared with the results based on ΔP_{top}, Fig. 10(b) shows that the void fraction prediction errors based on ΔP_{bottom} are larger than 10 % in almost the entire test range. The conditions with larger errors correspond to slug flow and bubble flow.

Based on one DP signal, the void fraction prediction errors for slug flow are a little larger than that for the other two flow patterns. Gas-liquid slug flow is one of the most complex flow patterns. Liquid slugs, small bubbles and large bubbles are heterogeneously distributed in the flow pipeline. The small bubbles coalesce into a large bubble and a large bubble may also be broken into many small bubbles, causing interface changes and complicated interaction between liquid and gas phases. It is generally thought that slug flow can result in a severe fluctuations of void fraction and pressure drop in the pipeline. Therefore, it is difficult to predict the void fraction depending only on one DP signal.

Void fraction estimation based on two DP signals

ΔP_{top} and ΔP_{bottom} are acquired from the top section and the bottom section of the Venturi tube, and hence mainly represent the sectional gas-liquid distribution and variation, respectively. Considering that void fraction is related to the gas-liquid distribution across the pipe, combining ΔP_{top} and ΔP_{bottom} will provide an entire liquid-bubble distribution and hence improve the void fraction prediction accuracy. It is necessary to build a connection between the void fraction and the optimal combination of the characteristic variables from Venturi DP signals.

ANN can adjust the weight value and the threshold value to build a map between input and output. Therefore, ANN can be a tool to build a bridge between the characteristic variables $d_{top}, d_{bottom}, R_{top}, R_{bottom}$ and the void fraction. The developed ANN model is the optimal combination of $d_{top}, d_{bottom}, R_{top}, R_{bottom}$ for void fraction estimation.

Based on ANN and $d_{top}, d_{bottom}, R_{top}, R_{bottom}$, the average relative error of void fraction estimation is 8.42%, and the relative errors of each sample is shown in Fig. 11.

From Fig. 11, it can be seen that the errors are closer to zero error line. The data in Table 1 present the proportion of the sample number in a given RE range to the total sample number. Table 1 shows that for most samples the void fraction prediction errors based on ΔP_{top} are lower than those based on ΔP_{bottom}. Combining ΔP_{top} and ΔP_{bottom} lowers the void fraction prediction errors.

In this work, the predicted samples come from 33 different working conditions, including 6 bubble flow, 8 plug flow and 19 slug flow situations. Fig. 12 illustrates the comparison of the void fraction estimation based on ΔP_{top}, ΔP_{bottom} and the combination of ΔP_{top} and ΔP_{bottom}.

From Fig. 12, it can be seen when the void fraction is less than 0.4, the estimation is satisfactory for different DP. While when the void fraction is larger than 0.4, the prediction errors distribute in a wide range based on either ΔP_{top} or ΔP_{bottom}. Combining ΔP_{top} and ΔP_{bottom} based on ANN improves the prediction accuracy for the majority of experimental samples.

Fig. 13 illustrates the void fraction prediction errors versus the mixture velocity of gas-liquid two-phase flow. In Fig. 13, the prediction errors based on ΔP_{top} mainly distribute within 10%, which is better than those based on ΔP_{bottom}. When the mixture velocity is small, the inertial force of the working fluid is weak and buoyancy is the dominant force. In this situation, bubbles move close to the top section of the pipe and ΔP_{top} induces the bubble distribution and movement directly. Meanwhile, ΔP_{top} hardly sense the information related to the liquid movement because the most area at the top section is occupied by bubbles. Therefore, the void fraction estimation based on ΔP_{top} is a little bit higher because of the scarcity of information for the liquid. ΔP_{bottom} induces bubble distribution and movement mainly by the fluctuation of the liquid flow in the bottom section of the pipe. This unclear connection between ΔP_{bottom} and the void fraction results in a relatively large prediction error for a small mixture velocity. When the mixture velocity is high, the inertial force of the working fluid is strong and the buoyancy force is weaker. Then, the bubbles move close to the axis of the pipe and either ΔP_{top} or ΔP_{bottom} induce only a part of the bubble distribution. Additionally, the high mixture velocity decreases the area occupied by the gas phase at the cross section of the pipe. Therefore, for the working condition with a high mixture velocity, the void fraction is underestimated, as shown in Fig. 13.

Table 2 presents the average relative errors of the void fraction prediction for different flow patterns. It is observed that the void fraction prediction based on ΔP_{top} is much better than that based on ΔP_{bottom} for bubble flow, which is accordant with the DP signal acquisition position. In bubble flow, the liquid is flowing in the pipe as the continuous phase, and the gas distributes almost homogeneously in the liquid as the dispersed phase along the upper pipe wall. Compared with ΔP_{bottom}, ΔP_{top} reveals much more information related to bubble distribution, which in turn results in a higher void fraction prediction accuracy. Combining ΔP_{top} and ΔP_{bottom} (based on ANN) reserves effective information and suppresses the information weakly related to the void fraction.

Fig. 14 illustrates the void fraction prediction errors based on ΔP_{top}, ΔP_{bottom}, and the combination of ΔP_{top} and ΔP_{bottom} using coloured bars. The corresponding reference void fraction, gas-liquid slip ratio, d_{top} and d_{bottom} for every experimental sample are also shown in Fig. 14. Fig. 14 shows that when the reference void fraction is higher than 0.4, the void fraction is underestimated for most working conditions using the method in this paper. Especially for a higher reference void fraction, the prediction error is much larger. A higher void fraction corresponds to a larger gas-liquid slip ratio. In this situation, a dominant gas flowing generates close to the axis of the pipe and the velocity of gas phase considerably exceeds that of the liquid phase. The larger velocity difference results in a small variation of gas-liquid phase interface and hence weakens the influence of bubbles on the liquid flowing. Because ΔP_{bottom} induces the bubbles mainly through the liquid flow, the void fraction prediction value based on ΔP_{bottom} is much lower and the prediction errors are noticeable, as shown in Fig. 14 with the green bars. In detail, for experimental samples 1-17 the liquid

flowrate ranges from 9.25 to 14.45 m^3/h with a slightly lower void fraction, and hence the gas-liquid slip ratios are relatively lower. The lower slip ratio means the velocity difference between gas and liquid phases is small. Then the influence of bubbles on liquid flowing is strong. In this situation, the void fraction estimation based on ΔP_{top} and ΔP_{bottom} is satisfactory. However for experimental samples 18-33, the liquid flowrate ranges from 3.73 to 7.91 m^3/h with a higher void fraction, and hence the slip ratios are relatively higher. Especially for experimental samples 18-28, the significantly higher gas-liquid slip ratios are one of the causes of void fraction underestimation and slightly larger prediction errors.

For experimental samples 18-33 in Fig. 14, d_{top} and d_{bottom} are larger than 1.2, while they are less than 1.2 for experimental samples 1-17. Comparing Figs. 5 and 6 and Fig. 14, it can be seen that experimental samples 18-33 are almost situated at the complex nonlinear section of Fig. 5-6 and the corresponding d_{top} and d_{bottom} are larger and scattered, which is another cause of a relatively larger prediction error. Experimental samples 1-17 almost locate at the near-linear section of Figs. 5 and 6 and the corresponding d_{top} and d_{bottom} are relatively smaller and concentrated, which results in a relatively smaller prediction errors. Additionally, for experimental sample 32, d_{top} and d_{bottom} are larger than 1.2 and the reference void fraction is near 0.4. This sample is outside both the near-linear and nonlinear areas in Figs. 5 and 6. The significant prediction error is due to the difficult match between the fluctuating index of DP signals and the void fraction for this sample. Combining ΔP_{top} and ΔP_{bottom} based on ANN, we can improve the prediction performance of this sample as shown in Fig. 14. However, a poor prediction for the samples away from or near the boundary of the training area is the general disadvantage of ANN, which makes the improvement for

this sample unsatisfactory. For sample 6, the void fraction is 0.6 and d_{top} is 0.9. For sample 7, the void fraction is 0.27 and d_{top} is 0.68. For sample 17, the void fraction is 0.52 and d_{top} is 0.65. These three samples are also close to the boundary of the training area as shown in Figs. 5 and 6, and hence the prediction error is a little bit larger.

The void fraction prediction results, whether based on ΔP_{top} or ΔP_{bottom}, are not satisfactory for the complex plug flow and slug flow. Combining ΔP_{top} and ΔP_{bottom} (based on ANN) also cannot improve the prediction accuracy for plug flow. From the view of ANN theory, the training samples for bubble flow and plug flow are less than that for slug flow, which is one of the reasons that the improvement of the void fraction prediction accuracy for bubble flow and plug flow is not as noticeable as that for slug flow. In other words, ANN could possibly build a better connection between inputs and outputs if there exist sufficient samples.

The generalization performance of ANN is good for the samples within the maximum scope of the training area, which is called the interpolation feature. However the extrapolation feature of ANN is worse. A few samples corresponding to bubble flow and plug flow scatter outside the training area, which decreases the void fraction prediction accuracy. This work could in future be extended to include vertical orientations and evaporating two-phase flows allowing validations with aforementioned works and current studies [18] [24], [29], [30].

CONCLUSIONS

This study proposes a new void fraction estimation method using two differential pressure (DP) signals acquired from one Venturi tube. The method adopts EMD to extract the fluctuating and stable variables of DP signals, and then adopts ANN to develop the map

between the extracted variables and the void fraction.

The study showed the extracted fluctuating index of DP signal from either top section or bottom section of the Venturi tube increases nearly linearly with increasing void fraction when void fraction is less than 0.4. When the void fraction is larger than 0.4, the relationship between the fluctuating index and the void fraction is complex. Therefore, the void fraction prediction performance is satisfactory under the conditions with a lower void fraction and a lower fluctuating index value of DP signal using the method proposed in this work. Under other conditions, the prediction error is relatively larger. The combination of ΔP_{top} and ΔP_{bottom} based on ANN can improve the prediction accuracy.

When gas-liquid mixture velocity is small, the inertial force of the working fluid is weak and buoyancy is the dominant force. The bubble distribution and movement is induced by ΔP_{top} and the liquid movement is suppressed. In this situation, the void fraction is overestimated based on ΔP_{top}. ΔP_{bottom} induces the bubble distribution and movement mainly by the fluctuation of the liquid flowing indirectly in the bottom section of the pipe, which results in a relatively large prediction error. The void fraction is underestimated when the mixture velocity is high because of the interaction between inertial force and buoyancy force.

When there is a high gas-liquid slip ratio there is in a large velocity difference between two phases and thus, a small variation of gas-liquid phase interface weakens the influence of bubbles on the liquid flow. Therefore, the void fraction is underestimated.

Compared with previous void fraction prediction methods based on DP signals, the method used in this work can estimate the void fraction using only two DP signals from one Venturi tube without the pipe pressure measurement before the Venturi tube and without any

coefficient determination prior to the online measurement. This significant simplification without compromising prediction accuracy is advantageous for measurement and analysis.

Acknowledgements

This work was supported by the National Natural Science Foundation of China (51304231), the Open Project Funding of State Key Laboratory of Industrial Control Technology (ICT170338), and the Shandong Provincial Natural Science Foundation, China (ZR2010EQ015).

Nomenclature

a,b,c	coefficients in Eq. (2)
ANN	artificial neural network(s)
c_j	pseudo-components in DP signal (Pa)
d	fluctuating index of DP signal
D	variance (Pa^2)
DP	differential pressure
EMD	empirical mode decomposition
F	fluctuating variable of DP signal (Pa)
$F_{top}, R_{top}, d_{top}$	F, R and d of DP signal from the top section of the Venturi tube
$F_{bottom}, R_{bottom}, d_{bottom}$	F, R and d of DP signal from the bottom section of the Venturi tube
IMF	instrinsic mode functions
$k_1(\alpha)$	empirical function in Eq. (1)
$k_2(\alpha)$	empirical function in Eq. (1)
l	index in Eq. (1)
m	number of the fluctuating components in DP signal
MSE	mean square error
n	number of the pseudo-components in DP signal
N	number of working conditions for void fraction prediction
$output$	calculated output of neural network model

p_f	fluctuating parameter
P	average pipe pressure (Pa)
Q_w	liquid flowrate (m^3 / h)
Q_g	gas flowrate (m^3 / h)
r	residual component of DP signal (Pa)
R	stable variable of DP signal (Pa)
RE	relative error
SD	standard deviation
$target$	desired output of neural network model
x_i	fluctuating component of DP signal (Pa)

Greek symbols

α	void fraction
ε	average relative error
ΔP_{bottom}	DP signal from the bottom section of the Venturi tube (Pa)
ΔP_{top}	DP signal from the top section of the Venturi tube (Pa)
ΔP_{TP}	average of DP signal (Pa)

REFERENCES

[1] Kawahara, A., Sadatomi, M., Okayama, K., Kawaji, M., and Chung, P.M.-Y., Effects of channel diameter and liquid properties on void fraction in adiabatic two-phase flows through microchannels, *Heat Transfer Engineering,* Vol. 26, no. 3, pp. 13-19, 2005. .

[2] Hewitt, G.F., and Burnout, G.H., *Handbook of Multiphase Systems*. Hemisphere, Washington DC, USA, 1982.

[3] Hosokawa, S., and Tomiyama, A., Bubble-induced pseudo turbulence in laminar pipe flows. *Int. J. Heat Fluid Fl.* Vol. 45, no. 21,, pp. 97-105, 2013.

[4] Sharaf, S., Silva, M.D., Hampel, U., Zippe, C., Beyer, M., and Azzopardi, B., Comparison between wire mesh sensor and gamma densitometry void measurements in two-phase flows. *Meas. Sci. Technol*., Vol. 22, no.10, pp. 1-13, 2011.

[5] Li, H.Q., *Two-Phase Flow Parameters Detection and Application*. Zhejiang Univ. Press, Hangzhou, China, 1991.

[6] Cioncolini, A., and Thome, J.R., Void fraction prediction in annular two-phase flow. *Int. J. Multiph. Flow,* Vol. 43, July, pp. 72-84, 2012.

[7] Celata, G.P., Cumo, M., Farello, G.E., Mariani, A., Solimo, A., Flow pattern recognition in heated vertical channels: steady and transient conditions. *Exp. Therm. Fluid Sci,.* Vol. 4, no. 6, pp. 737-746, 1991.

[8] Meng, Z.Z., Huang, Z.Y., Wang, B.L., Ji, H.F., Li, H.Q., and Yan, Y., Air–water two-phase flow measurement using a Venturi meter and an electrical resistance tomography sensor. *Flow Meas. Instrum.*, Vol. 21, no. 3, pp. 268-276, 2010.

[9] Srisomba, R., Mahian, O., Dalkilic, A.S., and Wongwises, S., Measurement of the void fraction of R-134a flowing through a horizontal tube. *Int. Commun. Heat Mass*, Vol. 56, August, pp. 8-14, 2014.

[10] Kim, S., Lee, J.S., Kim, K.Y., Kang, K.H., and Yun, B.J., An approximate formula for the capacitance–void fraction relationship for annular flows. Meas. Sci. Technol. Vol. 20, no. 12, 125404, pp.1-7, 2009.

[11] Uesawa, S.I., Kaneko, A., and Abe, Y., Measurement of void fraction in dispersed bubbly flow containing micro-bubbles with the constant electric current method. *Flow Meas. Instrum.,* Vol. 24, April, pp. 50-62, 2012.

[12] Jassim, E.W., and Newell, T.A., Prediction of two-phase pressure drop and void fraction in microchannels using probabilistic flow regime mapping. *Int. J. Heat Mass Tran.,* Vol. 49, no. 15, pp. 2446-2457, 2006.

[13] Lewis, S., Fu, W.L., and Kojasoy, G., Internal flow structure description of slug flow-pattern in a horizontal pipe. *Int. J. Heat Mass Tran.,* Vol. 45, no. 19, pp. 3897-3910, 2002.

[14] Milián, V., Esbrí, J.N., Ginestar, D., Molés, F., and Peris, B., Dynamic model of a shell-and-tube condenser. Analysis of the mean void fraction correlation influence on the model performance. *Energy*, Vol. 59, 15 September, pp. 521-533, 2013.

[15] Woldesemayat, M.A., and Ghajar, A.J., Comparison of void fraction correlations for different flow patterns in horizontal and upward inclined pipes. *Int. J. Multiph. Flow*, Vol. 33, no. 4, pp. 347-370, 2007.

[16] Fang, L.D., Zhang, T., and Jin, N.D., A comparison of correlations used for Venturi wet gas metering in oil and gas industry. *J. Petrol. Sci. Eng*., Vol. 57, no. 3, pp. 247-256, 2007.

[17] Lao, L.Y., *Two-Phase Flow Parameters Identification Method Research Based on the Dynamic Differential Pressure Signal*. Zhejiang Univ., Hangzhou, China, 1998.

[18] Bertoldi, D., Dallalba, C.C.S., and Barbosa, J.R., Experimental investigation of two-phase flashing flows of a binary mixture of infinite relative volatility in a Venturi tube. *Exp. Therm. Fluid Sci.,* Vol. 64, June, pp. 152-163, 2015.

[19] Steven, R., A dimensional analysis of two phase flow through a horizontally installed Venturi flow meter. *Flow Meas. Instrum*., Vol. 19, no. 6, pp, 342-349, 2008.

[20] Sun, B., Wang, E.P., Ding, Y., Bai, H.Z., and Huang, Y.M., Time-frequency signal processing for gas-liquid two phase flow through a horizontal Venturi based on adaptive optimal-kernel theory. *Chinese J. Chem. Eng*., Vol. 19, no. 2, pp. 243-252, 2011.

[21] Steven, R.N., Wet gas metering with a horizontally mounted Venturi meter. *Flow Meas. Instrum*., Vol. 12, no. 5, pp. 361-372, 2002.

[22] Zhang, H.J., Yue, W.T., Ma, L.B., and Zhou, H.L., Relationship between fluctuating differential pressure and void fraction of gas-liquid two-phase flow in Venturi tube. *J. Chem. Ind. Eng. (China),* Vol. 56, no. 11, pp. 2102-2107, 2005.

[23] Liu, X.D., Chen, Y.P., and Shi, M.H., Influence of gravity on gas–liquid two-phase flow in horizontal pipes, *Int. J. Multiph. Flow,* Vol. 41, May, pp. 23-35, 2012.

[24] Colin, C., Kamp, A., and Fabre, J., Influence of gravity on void distribution in two-phase gas-liquid flow in pipe. *Adv. Space Res.,* Vol. 13, no. 7-, pp. 141-145, 1993.

[25] Yeoh, G.H., Cheung, S.C.P., and Tu, J.Y., On the prediction of the phase distribution of bubbly flow in a horizontal pipe. *Chem. Eng. Res. Des*., Vol. 90, no. 1-, pp. 40-51, 2012.

[26] Huang, N.E., Shen, Z., Long, S.R., Wu, M.C., Shih, H.H., Zheng, Q., The empirical mode decomposition and the Hilbert spectrum for nonlinear and non-stationary time series analysis. *Proceedings of the Royal Society of London A: Mathematical, Physical and Engineering Sciences*, Vol. 454, no. 1971, pp. 903-995, 1998.

[27] Sun, B., *Gas-Liquid Two-Phase Flow Bi-Parameters Measurement Based on the HHT and SVM*. Zhejiang Univ. Hangzhou, China, 2005.

[28] Hornik, K., Stinchcombe, M., and White, H., Multilayer feedforward networks are universal approximators. *Neural Networks*, Vol. 2, no. 5, pp. 359-366, 1989.

[29] Godbole, P.V., Tang, C.C., and Ghajar, A.J., Comparison of void fraction correlations for different flow patterns in upward vertical two-phase flow, *Heat Transfer Engineering,* Vol. 32, no. 10, pp. 843-860, 2011.

[30] Thome, J.R., and El Hajal, J, Two-phase flow pattern map for evaporations in horizontal tubes: latest version, *Heat Transfer Engineering,* Vol. 24, no. 6, pp. 3-10, 2003.

Table 1 Void fraction prediction relative error distribution

	$\lvert RE\rvert < 5\%$	$5\% \le \lvert RE\rvert \le 10\%$	$\lvert RE\rvert > 10\%$
ΔP_{bottom}	32.35%	20.59%	47.06%
ΔP_{top}	38.24%	26.47%	35.29%
Combining ΔP_{top} and ΔP_{bottom}	41.18%	29.41%	29.41%

Table 2 Void fraction prediction errors for different flow patterns

	ΔP_{top}, ε	ΔP_{bottom}, ε	combination, ε
Bubble flow	**5.43%**	10.27%	6.69%
Plug flow	10.84%	**9.15%**	10. 24%
Slug flow	**11.17%**	14.01%	7.99%

List of figure captions

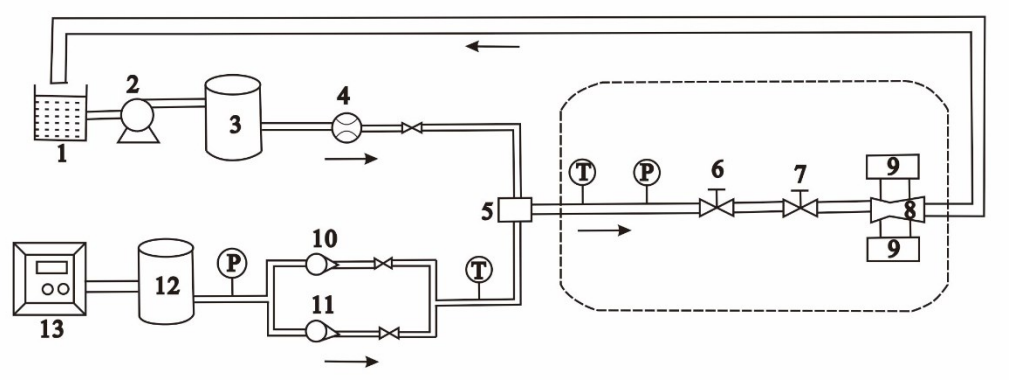

1 water tank 2 water pump 3 water surge tank 4 Electromagnetic flowmeter 5 mixer 6 valve 7 valve 8 Venturi 9 DP transducer 10 Vortex flowmeter 11 Rotameter 12 air surge tank 13 air compressor

Fig. 1 Schematic diagram of experimental facility

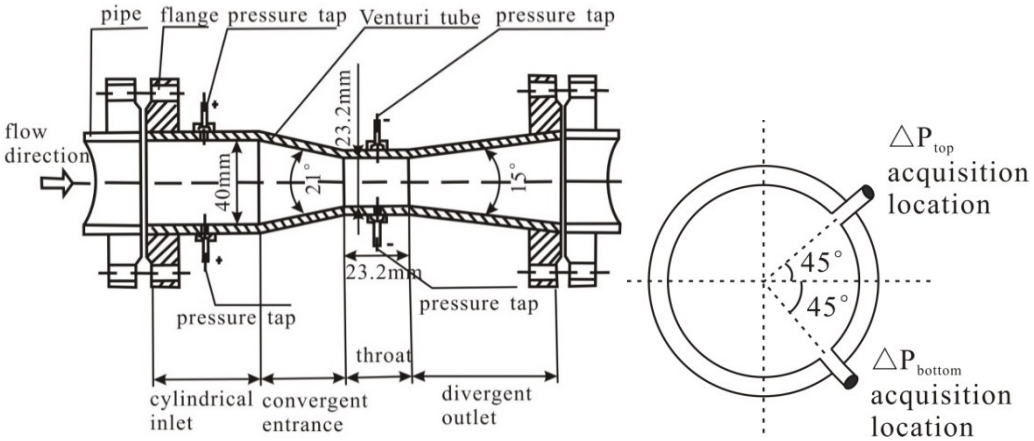

(a) **(b)**

Fig. 2 Locations for DP acquisition from Venturi tube

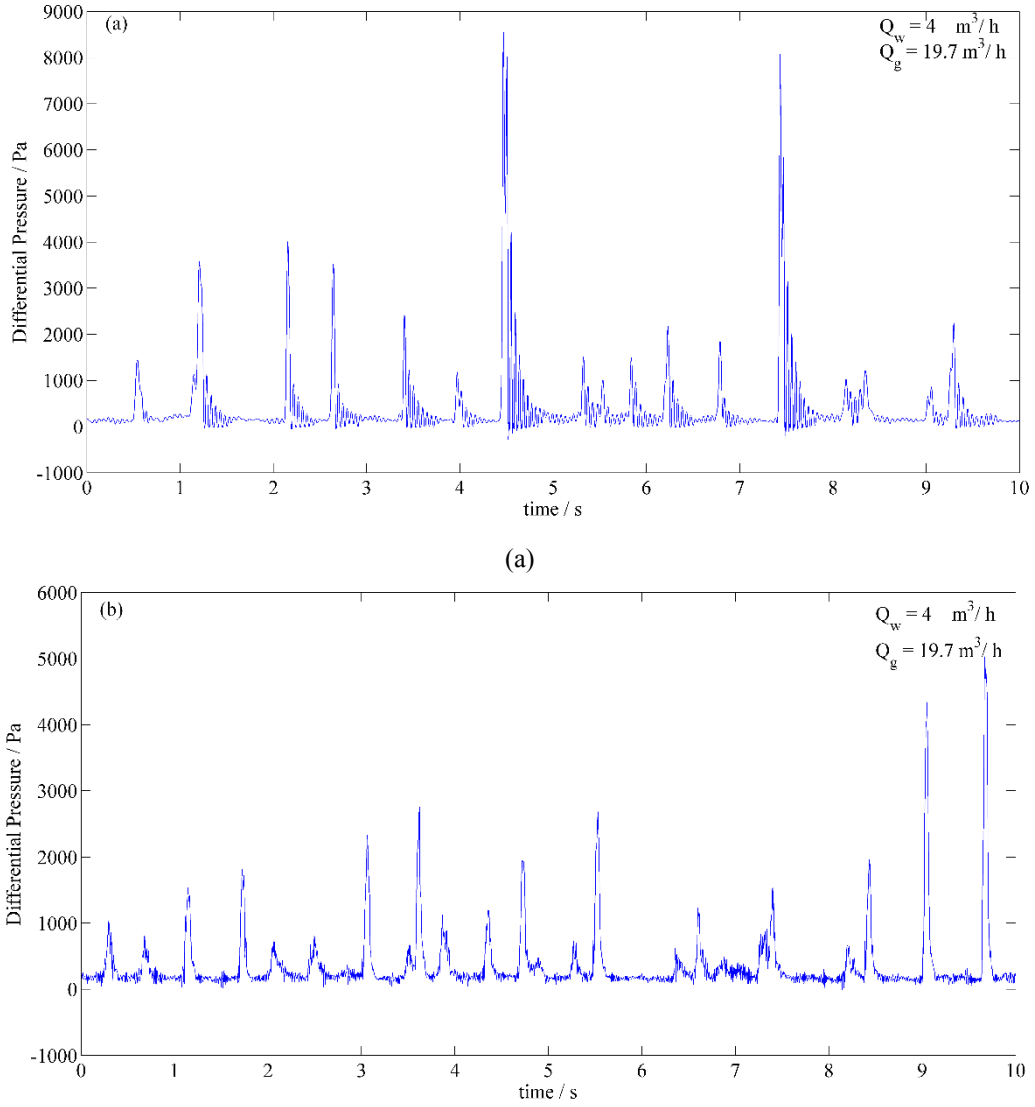

Fig. 3 DP signals from the Venturi tube (a) top section; (b) bottom section

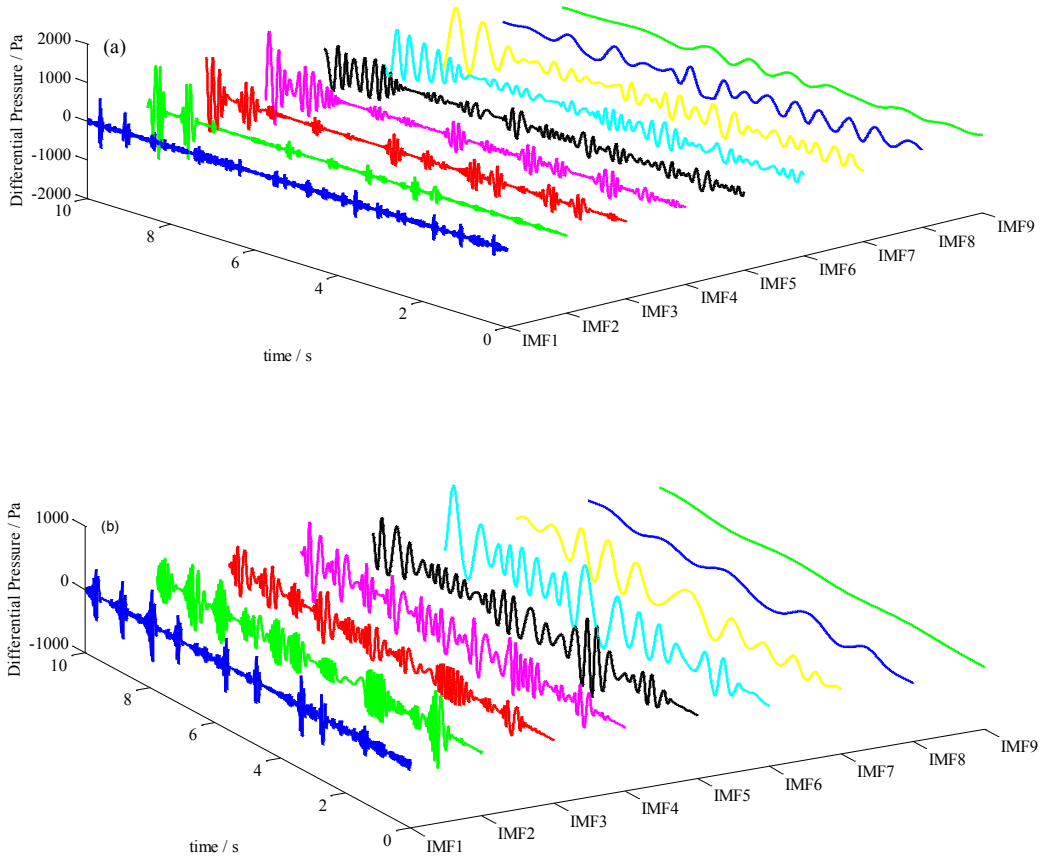

Fig. 4 IMFs of (a) ΔP_{top} and (b) ΔP_{bottom}

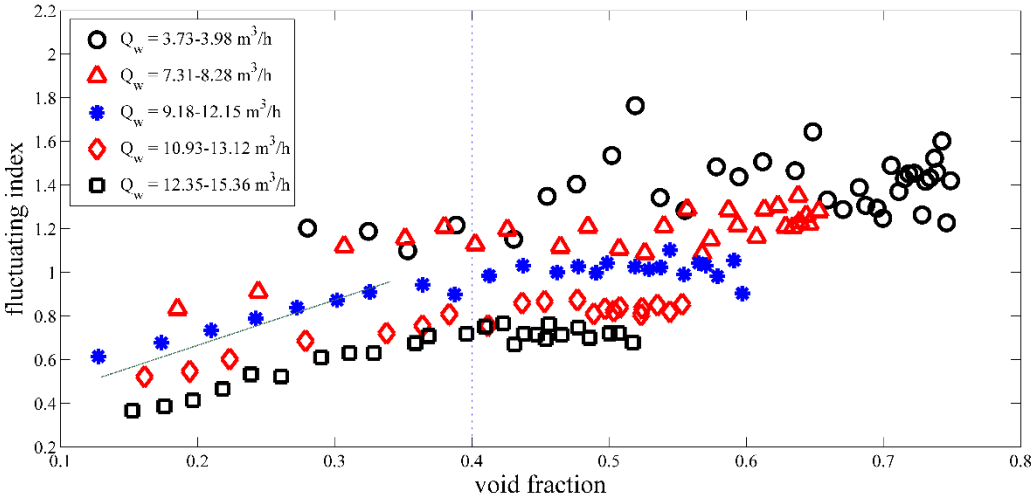

Fig. 5 Void fraction versus distribution of fluctuating index for DP from bottom section of Venturi

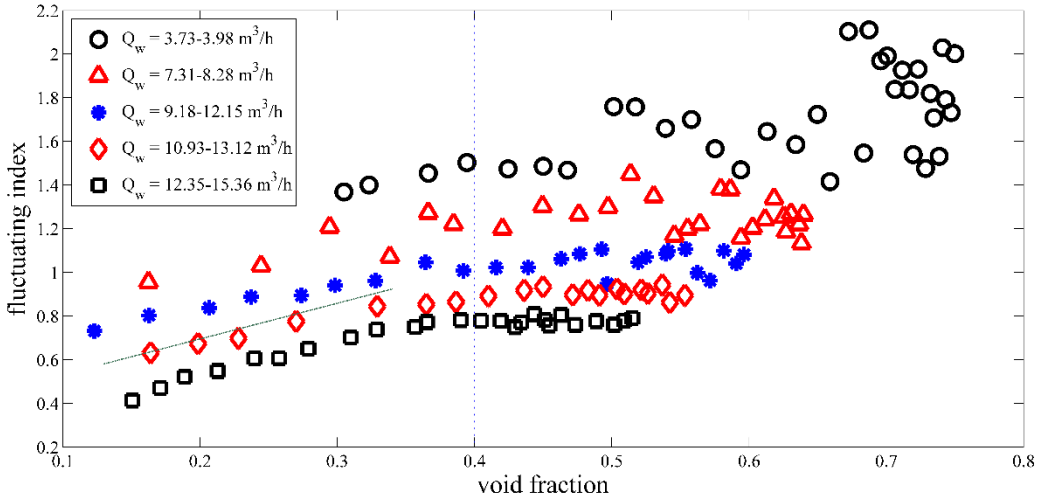

Fig. 6 Void fraction versus distribution of fluctuating index for DP from top section of Venturi

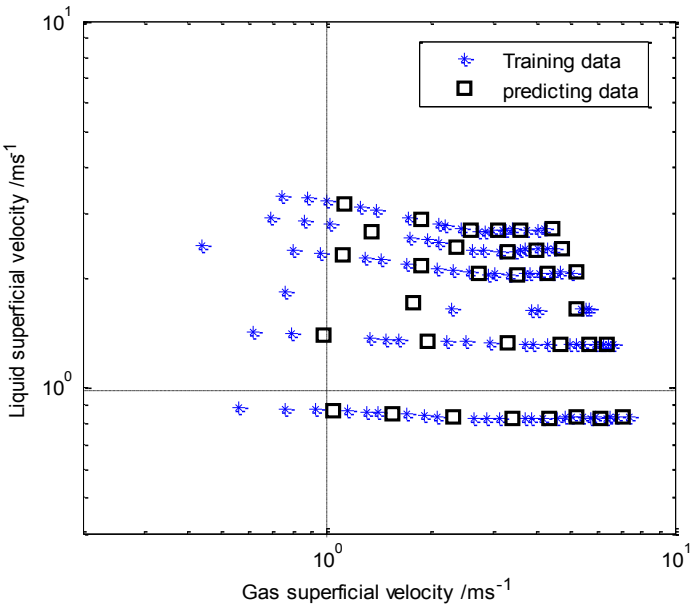

Fig. 7 Experimental working conditions

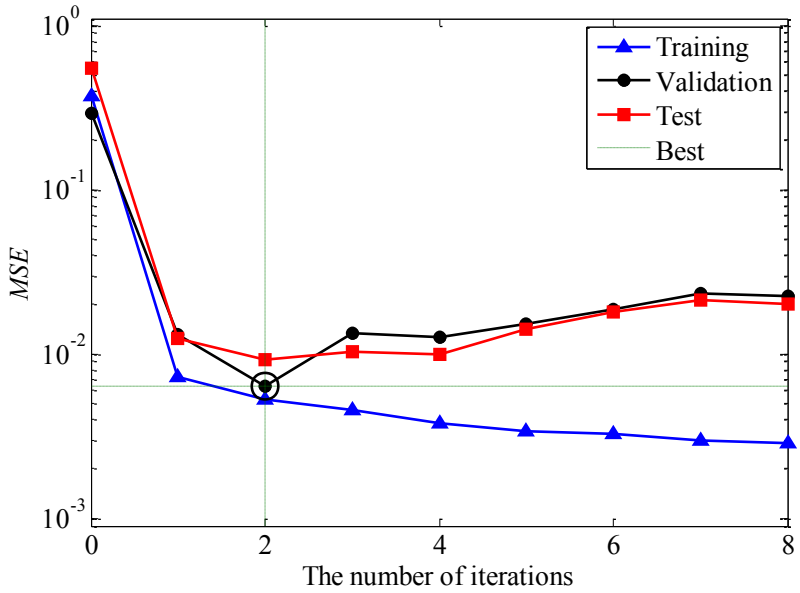

Fig. 8 Error change in ANN training process

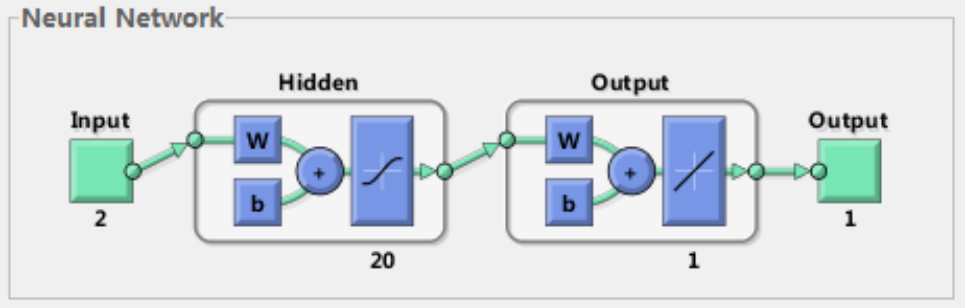

Fig. 9 Neural network structure

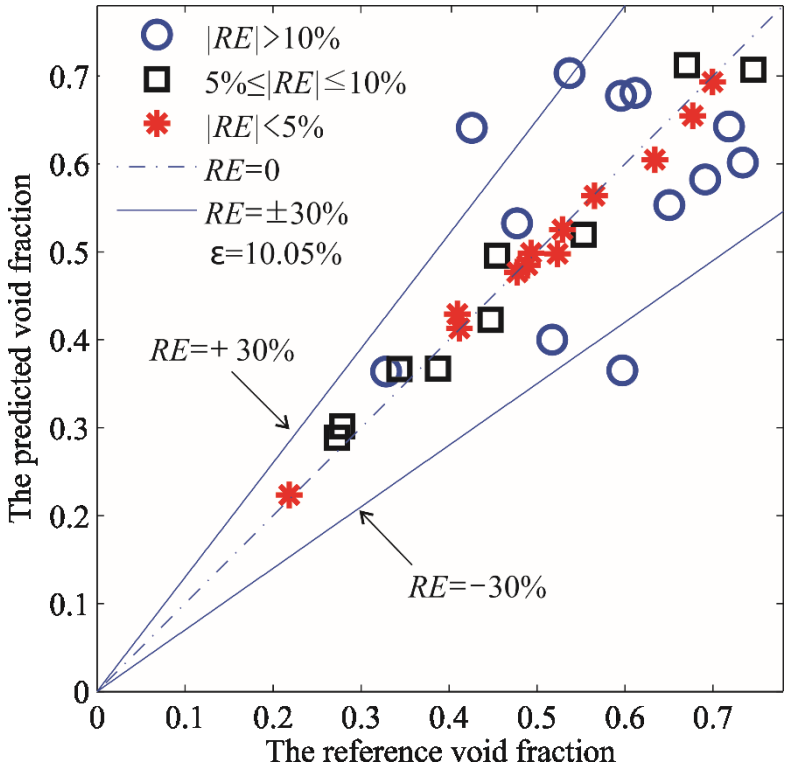

(a)

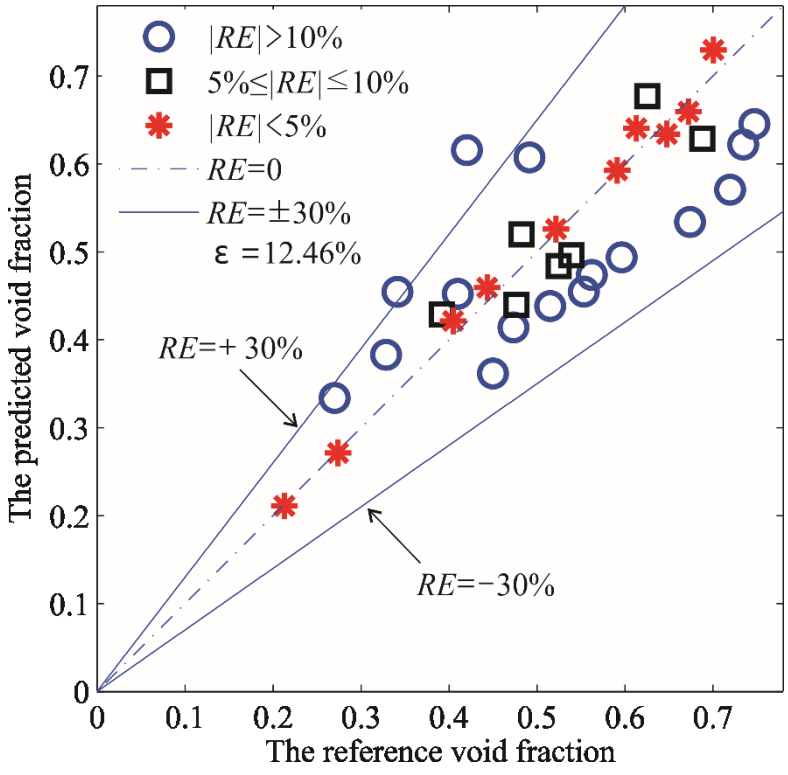

(b)

Fig. 10 Void fraction prediction results based on DPs (a) from top section (b) from bottom section

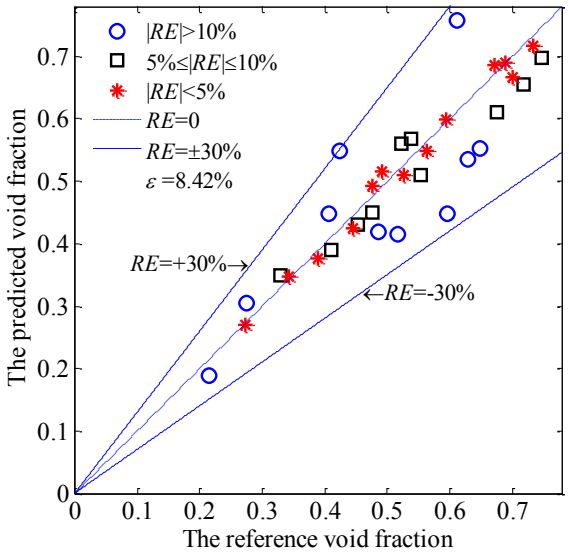

Fig.11 Void fraction prediction results based on ANN and two DP signals

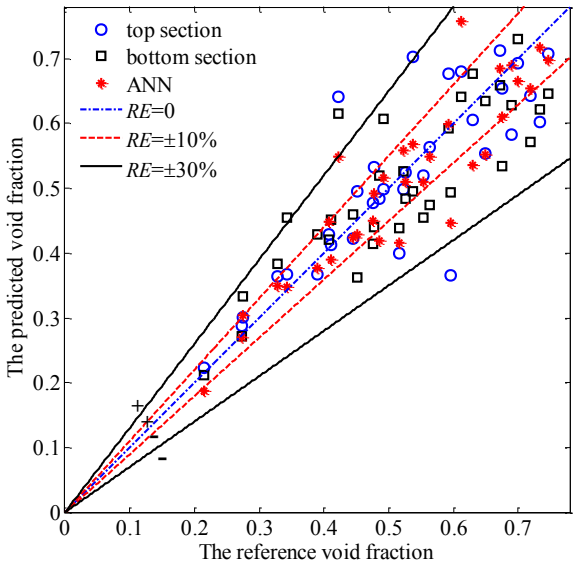

Fig.12 Void fraction prediction comparison based on different DP signals

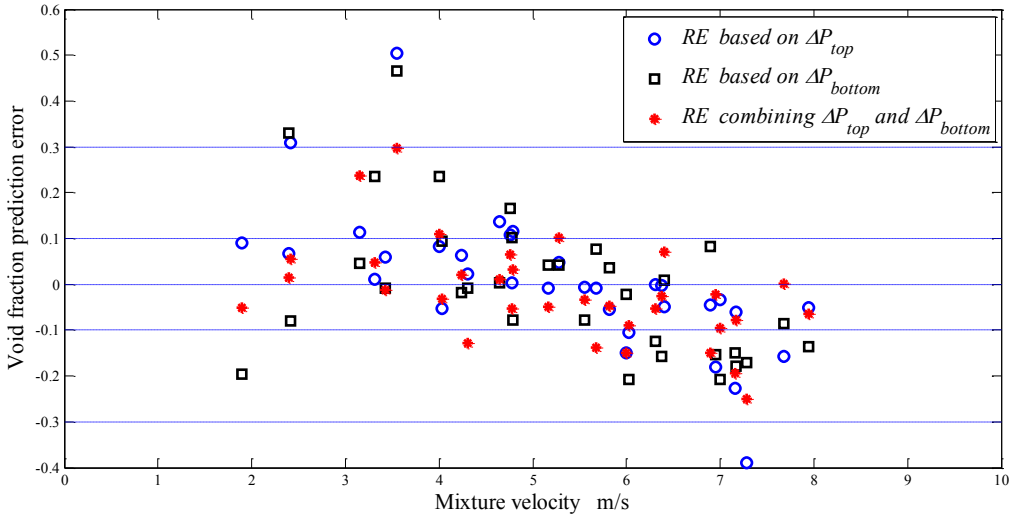

Fig.13 Void fraction prediction comparison

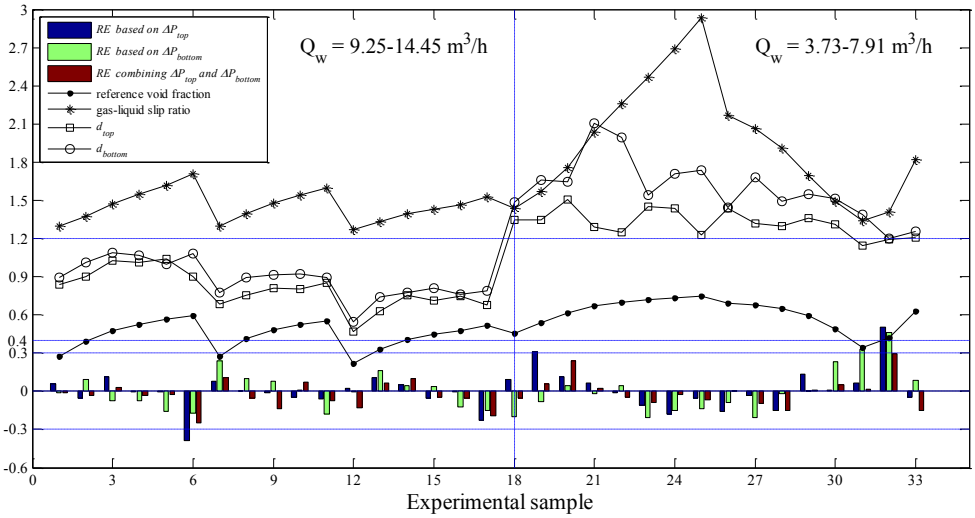

Fig.14 Working conditions and void fraction prediction error for individual experimental samples

Biographical details

Weiwei Wang is an associate professor of information and control engineering at China University of Petroleum (East China), Qingdao, China. She received her Ph.D. degree in industrial control technology from Zhejiang University, Hangzhou, China. Her current research interests include multiphase flow measurement and analysis, data mining and data fusion and signal processing.

Khellil Sefiane has MSc and PhD degrees in Chemical Engineering. He presently holds the Chair of Thermophysical Engineering at the University of Edinburgh. He is also ExxonMobil Fellow at the University of Edinburgh.In 2015 he was appointed Honorary Professor at Kyushu University.

Gail Duursma is a Lecturer in Chemical Engineering at the University of Edinburgh. She obtained her D.Phil. from the University of Oxford and after post-doctoral study at the University of Oxford, she joined the University of Edinburgh. She is a Member of the IChemE.

Xiao Liang is a Masters student of Engineering at the College of Information and Control Engineering, China University of Petroleum (East China), Qingdao, China. She is under the supervision of Prof. Weiwei Wang. Her current research interests are focused on two-phase flow measurement and signal processing.

Yu Chen is a Masters student of Engineering at the College of Information and Control Engineering, China University of Petroleum (East China), Qingdao, China. He is under the supervision of Prof. Weiwei Wang. His current research interests are focused on two-phase flow analysis and data fusion.